

# IRRADIATION OF SUPERCONDUCTING MAGNET COMPONENTS FOR FAIR

E. Mustafin<sup>#</sup>, E. Floch, A. Plotnikov, E. Schubert, T. Seidl, GSI Helmholtzzentrum für Schwerionenforschung, Planckstrasse 1, 64291 Darmstadt, Germany

L. Latysheva, INR RAS, 60th Oct. Anniversary Prospekt 7A, 117312 Moscow, Russia

A. Smolyakov, SSC RF ITEP, Bolshaya Cheremushkinskaya 25, 117218 Moscow, Russia

I. Strasik, GSI Helmholtzzentrum für Schwerionenforschung, Planckstrasse 1, 64291 Darmstadt, Germany on leave from FEI STU Bratislava, Slovak Republic.

## Abstract

In spring 2008 an irradiation test of superconducting magnet components was done at GSI Darmstadt in the frame of the FAIR project. Cave HHD with the beam dump of SIS synchrotron was used for irradiation. The irradiation set-up modeled a scenario of beam loss in a FAIR accelerator: U beam with energy of 1 GeV/u was used to irradiate a thin stainless steel bar at very small angle, so that the test samples situated behind the stainless steel bar were exposed to the beam of secondary particles created in the bar. The total number of U ions dumped on the target assembly was about  $2 \cdot 10^{14}$ . Presently, in spring 2009 some samples are still radioactive. In the paper we present the estimates of the energy deposition and secondary particle fluences in the test samples and also discuss some results of the irradiation campaign.

## EXPERIMENTAL SET-UP

The layout of the experimental set-up is schematically shown in Fig. 1 [1]-[3].

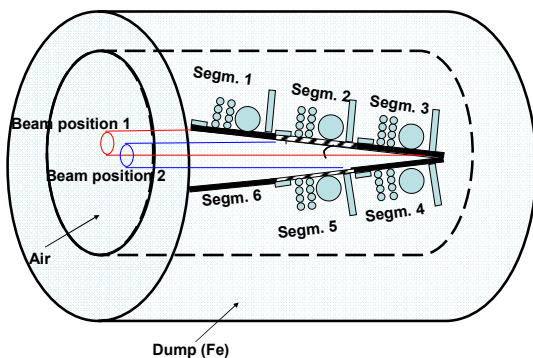


Figure 1: Layout of the experimental set-up.

The samples were organised into five identical segments. Each segment consisted of a 1 mm thick stainless steel plate and a set of thirteen samples. The arrangement of the samples in the segment is shown in Fig. 2. The segment 6 consisted of the stainless steel plate only and was used to study the residual activation induced in the plate [4]. Because of the expected high level of

neutron flux during the irradiation campaign, the target assembly was accommodated inside the SIS-18 synchrotron beam dump in Cave HHD of GSI Darmstadt. Because of the expected high level of neutron flux during the irradiation campaign, the target assembly was accommodated inside the SIS-18 synchrotron beam dump in Cave HHD of GSI Darmstadt.

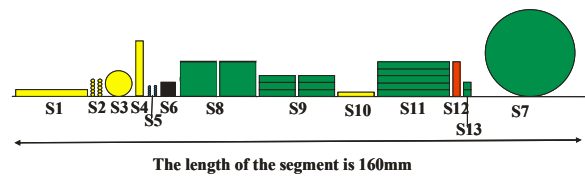


Figure 2: Layout of the samples in segments.

The following samples had been chosen for irradiation and were arranged in all five segments in identical way:

- S1 – stack of polyimide foils for thermal, mechanical, electrical tests and measurements by optical spectroscopy;
- S2 – pieces of kapton insulated wires;
- S3 – piece of nuclotron cable;
- S4 – piece of SIS300 cable;
- S5 – corrector conductor (piece of Cu-NbTi wire with enamel insulation);
- S6 – Super-FRS conductor;
- S7 – voltage breaker (sample S7 were present in Segments 2, 3, 4 and 5 only, it was absent in Segment 1);
- S8 – G11 rod for mechanical tests in compression mode;
- S9 – “dog-bone” shaped G11 plates for tensile tests;
- S10 – polyimide foils glued with Pixeo;
- S11 – G11 “sticks” for thermal conductivity tests;
- S12 – G11 plate for high voltage tests;
- S13 – temperature sensors

More detailed description of the samples (the geometry and the chemical composition) is given in [2].

The U beam of energy  $E = 1$  GeV/u irradiated the stainless steel plates under the grazing incidence of 2.38 degree so, that the samples S1-S13 were not directly exposed to the primary U beam particles but to the products of the nuclear reaction of U ions with the nuclei of the stainless steel plates. In this way a realistic scenario of the beam loss into the inner surface of the accelerator vacuum chamber was modelled. In order to accumulated

<sup>#</sup>e.mustafin@gsi.de

different radiation doses into the samples, the irradiation was done with two different positions of the U beam. In the first position the beam irradiated Segments 1, 2 and 3 and in the second position the beam irradiated Segments 2, 3 and 4. The beam had about Gaussian transverse distribution with r.m.s. sizes of about 1 cm in horizontal direction and 0.5 cm in vertical. The Segment 5 was irradiated with the beam tails only.  $1.06 \cdot 10^{14}$  ions were collected on the stainless steel plates in the first beam position and  $1.17 \cdot 10^{14}$  ions in the second beam position.

## COMPUTER MODELLING

There was no way to measure directly the energy deposited by the beam into the samples. The Monte-Carlo transport code SHIELD [5] was used to model the U beam interaction with the target assembly and to calculate the energy deposited into the samples.

The detailed dose distributions in the samples are given in [1] and [2]. Following [2], we show here the characteristic features of the dose distribution in two samples only: in samples S1 and S8.

Sample S1 is a stack of 10 layers of kapton foils. Each layer consists of 4 foils of different thicknesses: 0.012 mm, 0.025 mm, 0.05 mm and 0.1 mm. Computer simulation provides detailed estimates of energy deposited in the samples by different products of nuclear interaction of the U beam particles with the nuclei of the stainless steel plate. In Table 1 the energy deposition values are given for the first layer of samples S1 in the five different segments of the target assembly.

Table 1: Contribution of ion species to the energy deposition into the first layer of sample S1 (in MGy)

ion	Seg.1	Seg.2	Seg.3	Seg.4	Seg.5
$^1\text{H}$	0.023	0.17	0.23	0.13	0.039
$^2\text{H}$	$3.3 \cdot 10^{-3}$	$4.3 \cdot 10^{-2}$	$5.8 \cdot 10^{-2}$	$2.7 \cdot 10^{-2}$	$8.1 \cdot 10^{-3}$
$^3\text{H}$	$1.5 \cdot 10^{-3}$	$2.7 \cdot 10^{-2}$	$3.7 \cdot 10^{-2}$	$1.7 \cdot 10^{-2}$	$5.6 \cdot 10^{-3}$
$^3\text{He}$	$2.4 \cdot 10^{-3}$	$4.8 \cdot 10^{-2}$	$6.3 \cdot 10^{-2}$	$2.8 \cdot 10^{-2}$	$9.7 \cdot 10^{-3}$
$^4\text{He}$	$3.0 \cdot 10^{-3}$	$7.7 \cdot 10^{-2}$	0.11	$4.6 \cdot 10^{-2}$	$1.5 \cdot 10^{-2}$
$^7\text{Li}$	$7.7 \cdot 10^{-5}$	$1.1 \cdot 10^{-2}$	$1.4 \cdot 10^{-2}$	$5.2 \cdot 10^{-3}$	$2.3 \cdot 10^{-3}$
$^9\text{Be}$	$3.5 \cdot 10^{-5}$	$3.9 \cdot 10^{-3}$	$5.9 \cdot 10^{-3}$	$2.3 \cdot 10^{-3}$	$2.3 \cdot 10^{-4}$
$^{11}\text{B}$	$9.9 \cdot 10^{-5}$	$9.4 \cdot 10^{-3}$	$9.0 \cdot 10^{-3}$	$5.1 \cdot 10^{-3}$	$1.6 \cdot 10^{-3}$
$^{12}\text{C}$	$9.2 \cdot 10^{-5}$	$3.8 \cdot 10^{-3}$	$3.2 \cdot 10^{-3}$	$1.5 \cdot 10^{-3}$	$3.9 \cdot 10^{-4}$
Ion, Z=7-20	$3.3 \cdot 10^{-4}$	0.12	0.19	0.051	0.021
Ion, 21-40	0.01	1.18	1.59	0.61	0.22
Ion, 41-60	0.032	2.65	3.38	1.54	0.43
Ion, 61-91	0	0.046	0	0	0
Total	0.078	4.45	5.74	2.49	0.77

One may notice, that the fragments with charge numbers from Z=21 to Z=40 and from Z=41 to Z=60 make the major part of the energy deposition. The fragments with Z heavier than 61 are practically absent in the sample S1, because they are all stopped inside the stainless steel plate.

From the other hand one may notice in Table 2 that the number of heavy ion fragments penetrating into the first layer of samples S1 is negligibly small compared to the number of neutrons, protons and light fragments.

Table 2: Fluences of ion species penetrating into the first layer of sample S1 (in  $10^{13}/\text{cm}^2$ )

ion	Seg.1	Seg.2	Seg.3	Seg.4	Seg.5
n	7.17	73.2	100	53.1	14.7
$^1\text{H}$	2.79	21.9	29.2	15.5	4.06
$^2\text{H}$	0.46	8.22	10.8	4.73	1.24
$^3\text{H}$	0.25	5.51	7.65	3.38	0.85
$^3\text{He}$	0.14	2.55	3.23	1.44	0.41
$^4\text{He}$	0.15	4	5.54	2.32	0.6
$^7\text{Li}$	$7.6 \cdot 10^{-4}$	0.25	0.33	0.12	$3.4 \cdot 10^{-2}$
$^9\text{Be}$	$3.1 \cdot 10^{-4}$	$4.8 \cdot 10^{-2}$	$5.8 \cdot 10^{-2}$	$2.8 \cdot 10^{-2}$	$8.9 \cdot 10^{-4}$
$^{11}\text{B}$	$5.6 \cdot 10^{-4}$	$6.5 \cdot 10^{-2}$	$7.1 \cdot 10^{-2}$	$4.1 \cdot 10^{-2}$	$8.5 \cdot 10^{-3}$
$^{12}\text{C}$	0	$1.7 \cdot 10^{-2}$	$1.3 \cdot 10^{-3}$	$5.6 \cdot 10^{-3}$	$1.3 \cdot 10^{-3}$
Ion, Z=7-20	$6.8 \cdot 10^{-4}$	0.13	0.26	0.075	0.026
Ion, 21-40	$3.3 \cdot 10^{-3}$	0.2	0.22	0.094	0.027
Ion, 41-60	$2.5 \cdot 10^{-3}$	0.17	0.23	0.11	0.024
Ion, 61-91	0	$5.6 \cdot 10^{-4}$	0	0	0

Comparing the numbers in Tables 1 and 2 one may conclude, that the number of heavy ion fragments penetrating into the first layer of sample S1 is less than 1% compared to the total number of the secondaries penetrating into the layer, but the contribution of this small number of heavy fragments into the energy deposition is above 80% of the total deposited energy. This is because of the  $Z^2$ -dependence of the energy deposition on the charge number of the fragment.

The same picture one may observe looking into Tables 3 and 4, where the energy deposition and fluence values are given for the secondaries penetrating into the first layer (0.2 mm thick) of sample S8.

More detailed numbers for all samples are given in [1] and [2].

## RESULTS OF IRRADIATION

The irradiation test was done in May 2008 and after the irradiation the target assembly was stored in a 'lead-brick castle' to allow the residual activity to 'cool-down' to the

accessible level. First organic samples could be removed from the 'castle' after four month of 'cooling-down'. The samples with the metallic parts were removed after ten months after the irradiation. Some metallic parts are still in the 'castle' (one year after the irradiation) because they still show the residual dose rate at the level of 50  $\mu\text{Sv/h}$ . Purely organic samples show at the moment much lower level of residual activity: about 0.5  $\mu\text{Sv/h}$  and less.

Table 3: Contribution of ion species to the energy deposition into the first layer of sample S8 (in MGy)

ion	Seg.1	Seg.2	Seg.3	Seg.4	Seg.5
$^1\text{H}$	0.068	0.15	0.19	0.12	0.045
$^2\text{H}$	$1.4 \cdot 10^{-2}$	$3.5 \cdot 10^{-2}$	$4.4 \cdot 10^{-2}$	$2.4 \cdot 10^{-2}$	$8.2 \cdot 10^{-3}$
$^3\text{H}$	$8.0 \cdot 10^{-3}$	$2.3 \cdot 10^{-2}$	$2.8 \cdot 10^{-2}$	$1.6 \cdot 10^{-2}$	$5.4 \cdot 10^{-3}$
$^3\text{He}$	$1.5 \cdot 10^{-2}$	$4.0 \cdot 10^{-2}$	$4.9 \cdot 10^{-2}$	$2.6 \cdot 10^{-2}$	$9.4 \cdot 10^{-3}$
$^4\text{He}$	$2.3 \cdot 10^{-2}$	$6.8 \cdot 10^{-2}$	$8.2 \cdot 10^{-2}$	$4.4 \cdot 10^{-2}$	$1.6 \cdot 10^{-2}$
$^7\text{Li}$	$2.3 \cdot 10^{-3}$	$8.4 \cdot 10^{-3}$	$1.2 \cdot 10^{-2}$	$5.4 \cdot 10^{-3}$	$2.0 \cdot 10^{-3}$
$^9\text{Be}$	$5.2 \cdot 10^{-3}$	$2.6 \cdot 10^{-3}$	$3.4 \cdot 10^{-3}$	$1.2 \cdot 10^{-3}$	$5.7 \cdot 10^{-4}$
$^{11}\text{B}$	$1.0 \cdot 10^{-3}$	$4.9 \cdot 10^{-3}$	$6.5 \cdot 10^{-3}$	$3.3 \cdot 10^{-3}$	$8.2 \cdot 10^{-4}$
$^{12}\text{C}$	$7.4 \cdot 10^{-3}$	$2.7 \cdot 10^{-3}$	$5.0 \cdot 10^{-3}$	$1.6 \cdot 10^{-3}$	$8.8 \cdot 10^{-4}$
Ion, $Z=7-20$	0.027	0.11	0.14	0.043	0.021
Ion, 21-40	0.37	0.78	0.88	0.45	0.16
Ion, 41-60	0.87	1.67	1.77	0.83	0.28
Ion, 61-91	0.0032	0	0.035	0	0
Total	1.4	2.94	3.31	1.60	0.56

Table 4: Fluences of ion species penetrating into the first layer of sample S8 (in  $10^{13}/\text{cm}^2$ )

ion	Seg.1	Seg.2	Seg.3	Seg.4	Seg.5
n	26.5	67.1	88.9	53.8	20.7
$^1\text{H}$	8.97	20.3	25.5	15.7	5.68
$^2\text{H}$	2.69	7.15	8.84	4.54	1.61
$^3\text{H}$	1.7	4.97	6.26	3.05	1.13
$^3\text{He}$	0.81	2.19	2.71	1.35	0.54
$^4\text{He}$	1.18	3.62	4.43	2.19	0.811
$^7\text{Li}$	$4.7 \cdot 10^{-2}$	0.19	0.27	0.11	$4.5 \cdot 10^{-2}$
$^9\text{Be}$	$6.3 \cdot 10^{-3}$	$3.4 \cdot 10^{-2}$	$4.1 \cdot 10^{-2}$	$1.5 \cdot 10^{-2}$	$5.2 \cdot 10^{-3}$
$^{11}\text{B}$	$7.8 \cdot 10^{-3}$	$4.0 \cdot 10^{-2}$	$5.0 \cdot 10^{-2}$	$2.4 \cdot 10^{-2}$	$6.1 \cdot 10^{-3}$
$^{12}\text{C}$	$3.1 \cdot 10^{-3}$	$1.3 \cdot 10^{-2}$	$2.3 \cdot 10^{-3}$	$6.6 \cdot 10^{-3}$	$5.0 \cdot 10^{-3}$
Ion, $Z=7-20$	0.035	0.15	0.18	0.065	0.032
Ion, 21-40	0.057	0.11	0.14	0.068	0.026
Ion, 41-60	0.058	0.11	0.12	0.056	0.018
Ion, 61-91	$5.9 \cdot 10^{-5}$	0	$8.7 \cdot 10^{-4}$	0	0

In June 2009 first measurements of electrical and mechanical properties of the organic samples will start.

At the moment we may only report that the samples showed a visible sign of changes in dependence on the absorbed dose.

For example, in Fig.3 photos of samples S8 are shown.

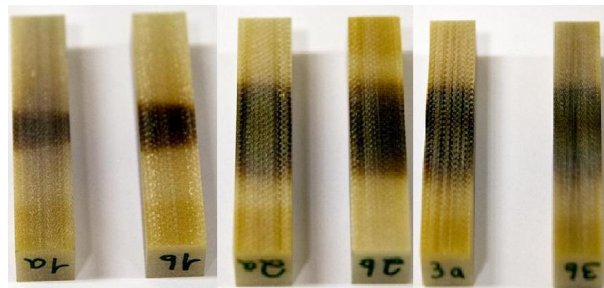


Figure 3: Photo of samples S8 from Segments 1, 2 and 3.

The burned areas on the samples correspond to the irradiated spots. One may see that the beam had an elliptical shape: the burned strip in Segment 1 is narrower than in Segments 2 and 3. According to the values in Table 3 samples S8 from Segments 1, 2 and 3 absorbed 1.4, 2.94 and 3.31 MGy respectively.

In Fig.4 samples S1 from all five segments are shown.



Figure 4: Photo of samples S1 from Segments 1-5.

Kapton foils showed weaker colorization compared to samples S8 made of G11. One may notice strong change of colour of samples S1 from Segment 5. Segment 5 was not exposed to the beam directly, only the projectiles from tails of Gaussian distribution of the beam in position 2 hit this segment. But it was found after the irradiation, that there was a narrow opening between the stainless plates of Segments 5 and 6. So, the U beam particles from the tail of the distribution penetrated through that narrow opening and hit samples S1 of Segment 5 directly. This illustrates once that heavy ions damage the organics much heavier compared to light particles.

The dose distribution was different not only in different segments but it also depended on the position of the samples relative to the stainless steel plate: samples situated closer to the plate received higher dose. This may be illustrated taking as an example samples S11 and comparing their colorization in dependence on the segment number and on the position of the G11 plates relative to the stainless steel plate. S11 consisted of five

G11 plates each of 1 mm thickness. In Fig.5 calculated dose values are shown for each of five plates depending on the segment and their position relative to the stainless steel plate: sample number on the axis x corresponds to the distance of the G11 plates to the stainless steel plate, G11 plates with smaller number were situated closer to the stainless steel plate.

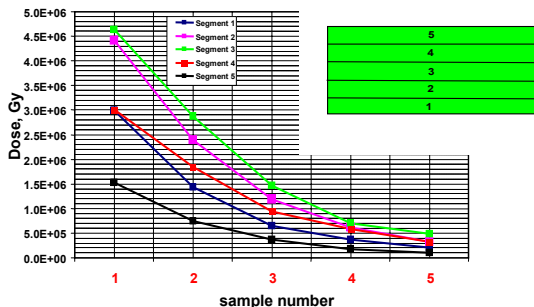


Figure 5: Calculated dose distribution in the center of samples S11 in different segments.

Dependence of the received dose on the distance from the stainless steel plate for samples S11 in one segment (Segment 2 in this case) is shown in Fig.6.

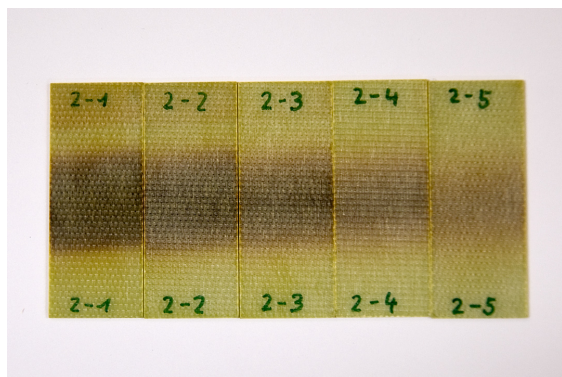


Figure 6: Dependence of the received dose on the distance of the samples from the stainless steel plate: first number on the G11 plate corresponds to the number of segment (Segment 2 in this case), the second number corresponds to the distance from the stainless steel plate (the G11 plate denoted as "2-1" was the closest to the stainless steel plate, and "2-5" was the most distant).

The dependence of the received dose on the segment is shown in Fig.7. The most left G11 plate is a pristine one (non-irradiated sample).

## CONCLUSION

High residual activation level doesn't allow yet measurement of changes in the electrical and mechanical

properties of irradiated samples in dependence on the received dose. First electrical and mechanical measurements are planned for June 2009.

At the moment we may only report that the samples showed clearly visible sign of radiation damage, namely a strong colorization ('burning') of the irradiated layers of the organic materials.



Figure 7: Dependence of the received dose on the segment: "1-1" is the first G11 plate of samples S11 in Segment 1, "2" – first plate of S11 in Segment 2, and "3-1", "4-1", "5-1" – first plates of S11 in Segments 3,4,5.

Calculations showed that the samples received doses up to few MGy. The distribution of sample colorization is in agreement with the calculated distribution of radiation damage.

## REFERENCES

- [1] L. Latysheva, "Irradiation experiment in Cave HHD: Numerical estimates of the energy deposition into the samples", GSI report DOC-2008-Nov-262-1, 2008.
- [2] L. Latysheva, "Contribution of the secondary particles to the dose distribution in samples S1 (1st layer) and S8 (1st part)", GSI report DOC-2009-Jan-47-1, 2009.
- [3] A. Plotnikov et al., "Preparation of the irradiation test at Cave HHD of GSI Darmstadt", poster contribution A3 to this conference.
- [4] I. Strasik et. al., "Depth-profiling of the residual activity induced by high-energy Uranium ions in thin stainless steel target", poster contribution A5 to this conference.
- [5] N.M. Sobolevskiy, "The SHIELD transport code: a tool for computer study of interaction of particles and nuclei with complex media", in: Proceedings of the Third Yugoslav Nuclear Society International Conference YUNSC 2000, Belgrade, October 2–5, 2000, The VINCA Institute, Belgrade, 2001, pp. 539–564